JOURNAL OF OPTOELECTRONICS AND ADVANCED MATERIALS, Vol. 12, No. 7, July 2010, p. 1515 - 1519

A comparative study of yttria stabilized zirconia coatings deposited with atmospheric plasma spray and detonation gun

N. PISTOFIDIS, G. VOURLIAS, D. CHALIAMPALIAS, E. PAVLIDOU,
K. CHRISSAFIS, G. STERGIOUDIS, E. K. POLYCHRONIADIS*
Physics Department, Aristotle University of Thessaloniki, 54124 Thessaloniki, Greece

One of the most promising materials for coating applications is Yttria stabilized Zirconia. In the present work, the structure and oxidation the resistance Yttria stabilized Zirconia coatings deposited with atmospheric plasma spray and detonation gun are examined. Both coatings have similar chemical composition and crystal structure. However, atmospheric plasma spray coatings are non-uniform due to the presence of dispersed pores and voids in the coating which do not communicate with each other and thus have insignificant effect on the coating protection. The detonation gun coating is more compact with lower porosity. In any case both of them have similar oxidation performance.

(Received April 22, 2010; accepted July 14, 2010)

Keywords: Ceramic coatings, Atmospheric Plasma Spray, Yttria stabilized Zirconia, Detonation-Gun

1. Introduction

Ceramic coatings are widely used for oxidation protection in high performance equipment such as turbine blades in power plants and jet engines, in order to increase the operational temperature and consequently the system efficiency [1]. Yttria stabilized zirconia (YSZ) has been chosen often for similar applications due to its low thermal conductivity, high thermal expansion coefficient and good oxidation resistance [2]. The deposition of this coating is usually accomplished with atmospheric plasma spraying (APS) [1]. Nevertheless for more demanding applications (such as engines fed with low quality fuels [3]) the properties of the coating have to be improved. Such an improvement could be achieved either with the application of different deposition methods or with the alteration of the coating composition. As far as it regards the deposition technique, spraying with detonation gun (D-Gun) could be an alternative [1]. This method is characterized by the formation of a detonation wave that results to the impact of the melted particles on the substrate surface at velocity of 800–1200 ms^{-1}. As a result the coating formed is more uniform and dense with high hardness and strong adhesion to the substrate [4].In the present work the morphology of these coatings is compared. Their structure is also examined but in lower extend. However the main target is the estimation of the oxidation behavior of each coating and its correlation with the observed morphology and structure. In any case, important information was gathered, which could be useful to the selection of the suitable material for applications under similar conditions.

2. Experimental

The coatings were deposited onto a Ni-base superalloy plate with nominal composition (% wt) 55 Ni, 22 Cr, 21 Co and 1 Al and dimensions 25x50x2.5 (mm). Prior to the deposition, the surface of the substrate was grit-blasted using 300 μm alumina grit, in order to remove residual oxide impurities and to increase its roughness, both aiming to achieve better adhesion between the metallic substrate and the ceramic coating. As it was already mentioned, the coatings were deposited with APS and D-gun respectively. For APS the plasma gas was an Ar mixture with He, with a total flow rate of 50 l/min. The current intensity was 530-550 A and the power supply about 30 kW. The powder-feeding rate was 20 g/min, while the gun was kept in a distance of 120 mm from the surface to be coated. For the D-gun, the C_2H_2:O_2 ratio was 1:1.03-1.08, the detonation frequency was 4-6 shot/s, the powder flow rate 18-54 g/min and the distance between the target and the gun 80-120 mm. The powder used in both cases was composed by agglomerates of nanoparticles with composition of ZrO_2-8mol% Y_2O_3 [5-6]. After the coating deposition, the as-coated samples were cross-sectionally cut, mounted in bakelite and polished up to 5 μm alumina emulsion for their study with scanning electron microscopy (SEM) using a 20 kV JEOL 840A SEM. SEM was also used for the observation of the surface of the coupons without any preparation. The structural characterization of the coatings was accomplished with conventional and high resolution electron microscopy (CTEM, HREM) using a 100 kV JEOL 100CX TEM and a 200 kV JEOL 2010 HREM, after the necessary preparation of the examined samples, as well as with X-Ray Diffraction (XRD) using a Siemens

D-8000 diffractometer with CuKα radiation, where the samples were examined after progressive polishing. The later enables the collection of information from different layers through the whole thickness of the coating. Finally, the oxidation resistance of the examined coatings (after detached from the metallic substrate) was evaluated with Thermogravimetric Analysis-Differential Thermal Analysis (TG-DTA) with a Setaram SETSYS TG-DTA system, which allowed non-isothermal heating of the specimens up to 1500°C, in a 50 ml/min flow of air.

3. Results

3.1. Characterization of the YSZ coating deposited with APS

A large amount of elementary informati0on for the coating could be gathered from the SEM examination of its cross-section. The SEM micrograph of Fig. 1 reveals that the coating deposited with APS is non-uniform due to the presence of dispersed pores and voids with different sizes and shapes in its mass. Furthermore these formations are not uniformly distributed in the coating, but in certain areas they form clusters, while in others the material is very compact.

This phenomenon is not peculiar and it is triggered by the deposition method [1]. Actually, it is an inherent characteristic of APS coatings because not only liquid but also partially molten or even solid YSZ droplets reach the surface of the already formed coating, which is more or less solid. Solidification of the droplets is due to fast cooling during their flight. The solid material is incorporated in the coating with very small changes of its shape. Thus, it may not fit exactly to the existing surface morphology and as a result pores are created. Moreover, poor wetting of the already deposited is possible resulting in poor adhesion, which leads to the formation of voids during cooling because of shrinkage [7].

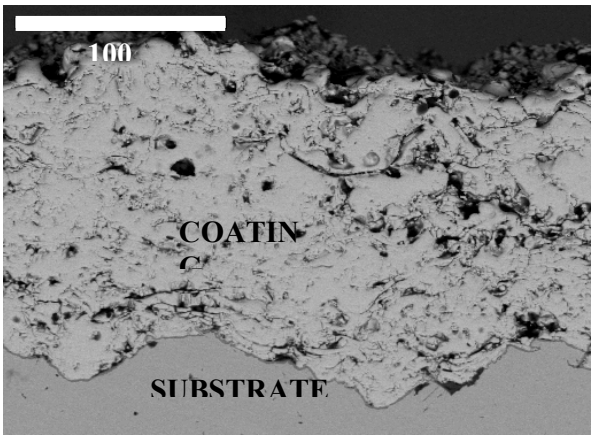

Fig. 1. SEM micrograph of the cross-section of the YSZ coating deposited with APS.

Analyzing the YSZ powder with XRD analysis it was found that it is composed of the tetragonal YSZ phase (Fig.2a). Furthermore, using the Scherrer formula [6, 8] it was revealed that the powder is consisted of nanosized grains. Thus, it is expected that the small grain size would contribute significantly to the restriction of the coating porosity [7]. However, in the cross sectional micrograph of the as deposited coating (Fig. 1) a remarkable elevated percentage of porosity is illustrated. This phenomenon is attributed to the incorporation of the nanograins in the donor material before the deposition process leading to the formation of larger grains which average diameter is 20μm (Fig. 2b, 2c). Furthermore, an additional incorporation procedure takes place during the deposition process. This progressive incorporation results to the formation elevated size grains and finally to the creation of high porosity percentage. In any case, as the pores do not form a network, it is not likely to facilitate oxidation. By contrast, their presence in some cases is favorable since heat transfer is more difficult through a gaseous phase and consequently they increase the thermal barrier effect of the ceramic coating [8,9]. However when the coating fails, it is certain that they will accelerate the coating decomposition because they reduce the mechanical strength of the ceramic phase.

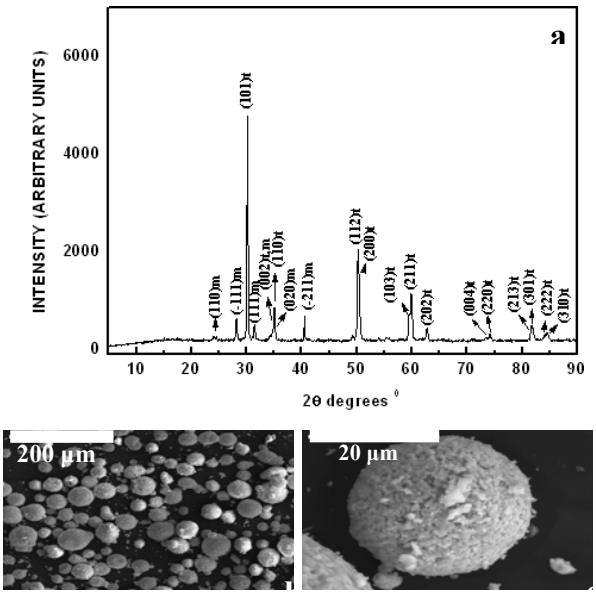

Fig. 2. XRD pattern (a) of the feedstock (tetragonal-ZrO_2, monoclinic-ZrO_2) and SEM micrographs of the initial feedstock powder material (b: at low magnification, c: at higher magnification focused on the surface of the framed area).

However, more interesting would be the examination of the cross-section of the coating without polishing along a fracture surface, which is presented in the SEM micrograph of Fig.3. The examination of this surface is important because YSZ is very brittle and as a result during fracture its crystals are separated along their

boundaries without any significant deformation. Thus, the images taken from the fracture surface offer a three-dimensional overview of the crystals composing the coating.

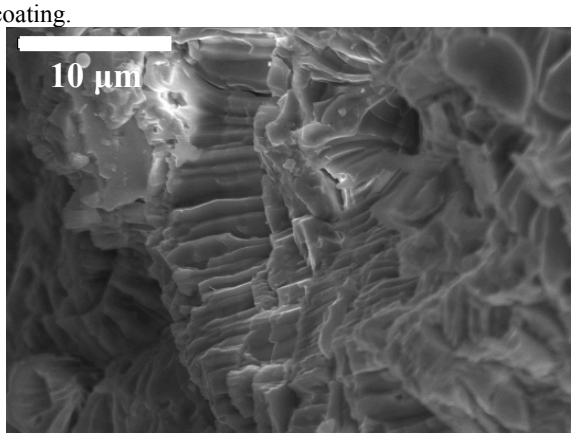

Fig. 3. SEM micrographs of the fracture surface of the YSZ coating deposited with APS.

In any case, in Fig. 3 rather complicated morphology is observed. First of all, columnar formations are predominant with growth direction perpendicular to the substrate (following the heat flow). These formations seem to compose larger plate-like bodies, which could be considered as lamellas when examined at lower magnification. Obviously each lamella is formed through the solidification of a droplet of the feedstock. Furthermore, some spherical formations are also distinguished, which are very likely to originate from partially molten particles of the feedstock. These formations are composed from adequate sized crystals grains, as the bright field TEM micrograph of Fig. 4 shows [10].

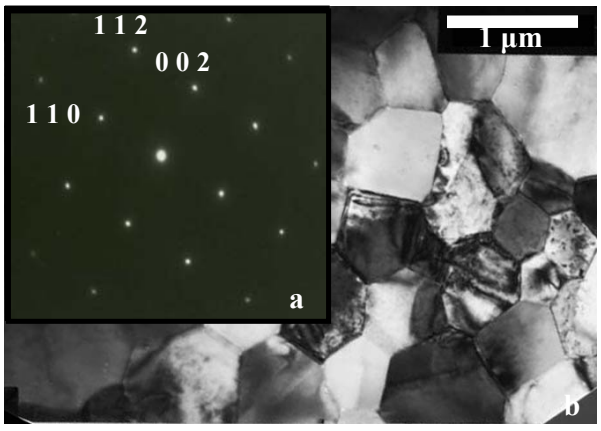

Fig. 4. Bright field TEM micrograph (a) of the YSZ coating deposited with APS along with electron diffraction patterns (b) referring to tetragonal ZrO_2.

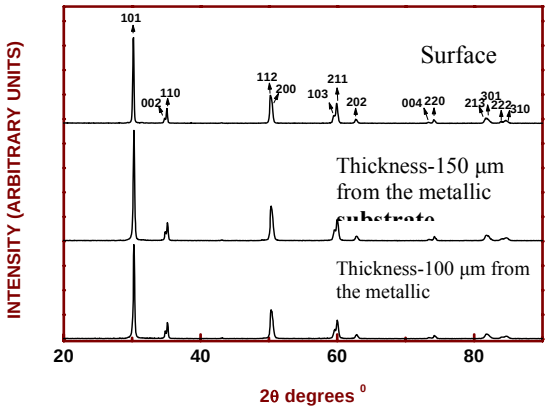

Fig. 5. XRD pattern from different depths of the YSZ coating deposited with APS referring to ZrO_2- 8 mol% Y_2O_3.

In order to examine the coating structure, XRD was used combined with progressive grinding so as to examine the coating in its whole depth. Its thickness (about 150 to 200 μm) does not allow the X-rays to penetrate into the coating and as a result only the upper part could be examined. For this reason after the initial examination, the coating was polished to a depth of about 50 μm and the as formed surface was re-examined. This process was repeated twice, in order to examine even the layers close at the ferrous substrate. The XRD patterns (fig.5) indicate, beyond any doubt, that the coating is exclusively composed by tetragonal crystals of YSZ with composition of ZrO_2-8mol% Y_2O_3 regardless the examined depth. Hence, although the coating morphology is rather variable, its structure (and chemical composition) is very uniform. This conclusion is rather interesting because it implies that the coating is free from inclusions or other elements that could initiate or facilitate oxidation. Furthermore, the presence of tetragonal crystals is favorable for the oxidation resistance, because they are more stable compared to monoclinic crystals [10].

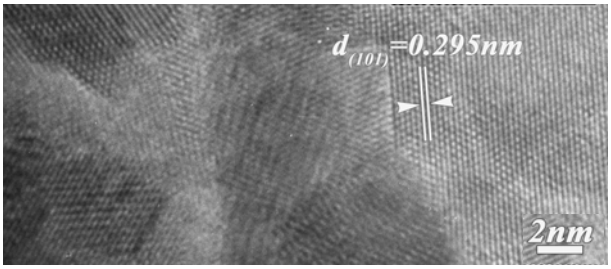

Fig. 6. HREM micrograph of a nanocrystalline area of the YSZ coating deposited with APS. The lattice planes of ZrO_2 are indicated on the HREM micrograph.

From Fig. 4 it was found that the coating is mainly composed of large sized crystals.

However, the fact that fast cooling takes place during deposition renders the formation of nanocrystals possible. For this reason the coating was also examined with HREM. A micrograph is presented in Fig. 6 where nanocrystals are observed with an average size less than 10 nm. In any case, their formation is random and they refer to a very small fraction of the coating and hence, their effect on the oxidation behavior could be neglected.

3.2. Characterization of the YSZ coating deposited with D-Gun

When D-gun is used for the coating growth, the maximum temperature of detonation torch is typically 3500–4500°C, much lower than that of the APS flame (>5000°C). Furthermore, the heating time for particles in the detonation torch is very short and the heat transfer between the detonation wave and the particles is rather limited, because of the high velocity [4]. Therefore, it is difficult to melt the YSZ ceramic particles (T_m=2600°C [11]) during detonation spraying. To avoid the presence of unmelted particles in the gun stream the C_2H_2:O_2 ratio was adjusted at 1:1.03-1.08 in order to obtain high temperature flame.

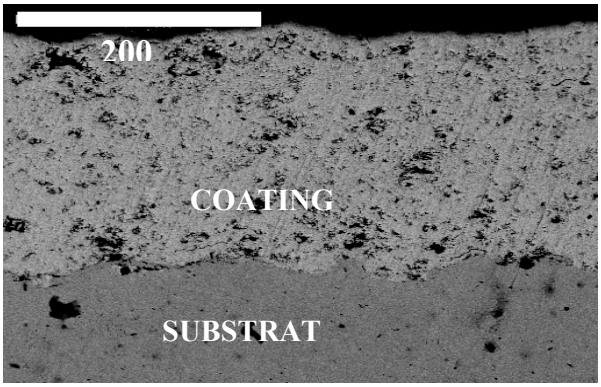

Fig. 7. SEM micrograph of the cross-section of the YSZ coating deposited with D-gun.

The morphology of the cross-section of the coating, as it is presented in Fig. 7, it is very characteristic. In this case a more compact deposition is revealed with fewer pores, voids and microcracks compared to the coating deposited with APS. Obviously this phenomenon is due to the fact that the droplets of YSZ which are formed with D-gun are more uniform, as far as it regards their physical state [10]. When APS was used for the coating deposition, the YSZ particles exiting the torch are totally or semi molten, while due to the fast cooling during their flight their solidification was also possible. However, the D-gun produces a stream of droplets which are more or less the same [10]. The later, along with the high collision speed of the D-gun, results in better fitting of the feedstock on the surface of the substrate.

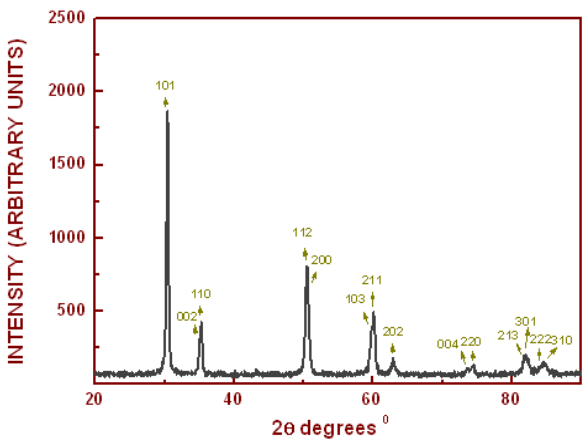

Fig. 8. XRD pattern of the YSZ coating deposited with D-gun referring to ZrO_2- 8 mol% Y_2O_3.

The XRD pattern (Fig. 8) coming from the D-Gun YSZ coating, is similar with the pattern of the APS coating (Fig. 4). Thus, although the morphology of the examined coatings is rather different, the structure and the chemical composition remains the same in both cases.

3.3. Oxidation performance

The previous analysis about the structure of the coatings and their morphology implies good oxidation resistance. Indeed, the D-gun coating is rather compact and in the APS coating the existing pores and voids do not form any network that could facilitate the diffusion of aggressive ionic species towards the substrate, as it was already mentioned. Further-more, the microscopical analysis along with the XRD patterns verifies sufficient crystal growth, while the formation of nanograins is rare. These facts support the hypothesis that the oxidation resistance of the coatings would be satisfactory because there exist fewer grain boundaries which facilitate significantly the corrosion process. To verify this hypothesis, TG-DTA was used in atmospheric air by applying non-isothermal heating up to 1500°C.

For the specimen coated with APS the results are summarized in the plots of Fig. 9. It is obvious that the mass of the sample does not change with regard to the exposure time up to the temperature examined. The same plot characterizes the sample coated with D-gun. Hence none of the YSZ coatings decomposes up to 1500°C. Furthermore, both of them are impermeable enough to protect the metallic substrate. For this reason there are no significant differences between the appearance of the two coatings before and after heating. Consequently they are both effective under the conditions studied.

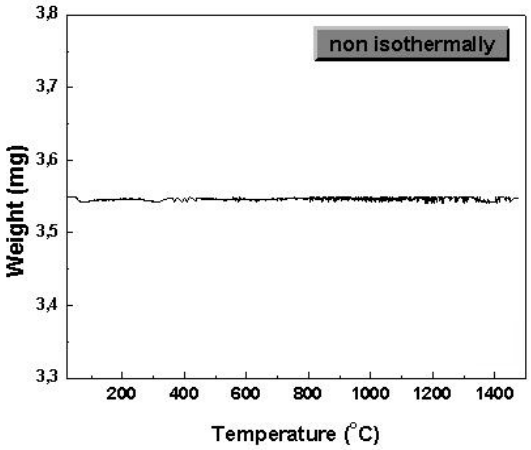

Fig. 9. Thermogravimetric plot of the mass change per unit of surface for the YSZ coating deposited with APS (up to 1500°C).

4. Conclusions

The microscopical and XRD analysis of the YSZ coatings deposited with APS and D-gun showed that both of them have similar crystallographic and chemical characteristics. This is not peculiar, given that the same material was deposited in each case. However there are differences on their morphology, as far as it concerns the porosity of each coating, which could be attributed to the different deposition method. However, these differences do not affect their oxidation resistance which was verified with TG-DTA. This method proved that both YSZ coatings are suitable for applications in atmospheric air up to 1500°C.

References

[1] T. A. Taylor, ‘’Ceramic Coatings’’, ASM Handbook, Vol. 5 (2002).
[2] R. L. Jones, C. E. Williams, Surf. Coat. Techn. **32**, 349 (1987).
[3] S.Y. Park, J. H. Kim, M. C. Kim, H. S. Song, C. G. Park, Surf. Coat. Techn. **190**, 357 (2005).
[4] Y. N. Wu, F. H. Wang, W. G. Hua, J. Gong, C. Sun, L. S. Wen, Surface and Coatings Technology, **166**, 189 (2003).
[5] W. B. Gong, C. K. Sha, D. Q. Sun, W. Q. Wang, Surf. Coat. Techn. **201**, 3109 (2006).
[6] R. S. Lima, A. Kucuk, C. C. Berndt, Mat. Sci. Eng. A, **313**, 75 (2001).
[7] A. Kulkarni, A. Vaidya, A.. Goland, S. Sampath, H. Herman, Mat. and Eng. A, **359**, 100 (2003).
[8] J. F. Li, H. Liao, X. Y. Wang, C. Coddet, H. Chen, C. X. Ding, Th. Sol. Fil., **460**, 101 (2004).
[9] H. Chen, X. Zhou, C. Ding, J. Eur. Cer. Soc. **23**, 1449 (2003).
[10] R. McPherson, Surf. Coat. Tech., **39/40**, (1989).
[11] CRC Handbook of Chemistry and Physics, CRC Press, London, (1999-2000).

*Corresponding author: polychr@auth.gr